JOURNAL OF MATERIALS SCIENCE **38** (2003) 633–642

Correlation of fatigue and creep crack growth in poly(vinyl chloride)

Y. HU
Department of Macromolecular Science, and Center for Applied Polymer Research, Case Western Reserve University, Cleveland, OH 44106-7202, USA

J. SUMMERS
PolyOne Corporation, Avon Lake, OH 44012, USA

A. HILTNER*, E. BAER
Department of Macromolecular Science, and Center for Applied Polymer Research, Case Western Reserve University, Cleveland, OH 44106-7202, USA
E-mail: pah6@po.cwru.edu

Slow crack growth in PVC pipe was studied in order to develop a methodology for predicting long-term creep fracture from short-term tension-tension fatigue tests. In all cases, the crack propagated continuously through a crack-tip craze. In fatigue, the density of drawn craze fibrils gradually increased with decreased frequency and increased temperature. At the lowest frequency, 0.01 Hz, the fibril density in fatigue approached that in creep. The kinetics of fatigue and creep crack growth followed the conventional Paris law formulations with the same exponent 2.7, $da/dt = A_f \Delta K_I^{2.7}$, $da/dt = BK_I^{2.7}$, respectively. The effects of frequency, temperature and *R*-ratio (the ratio of minimum to maximum stress intensity factor in the fatigue loading cycle) on the Paris law prefactors were characterized. Comparison of frequency and *R*-ratio tests revealed that the fatigue contribution depended on strain rate. Therefore, at each temperature, crack growth rate was modeled as the product of a creep contribution that depended only on the maximum stress intensity factor and a fatigue contribution that depended on strain rate: $(da/dt) = BK_{I,\max}^{2.7}(1 + C\dot{\varepsilon})$, where B is the prefactor in the Paris law for creep and C is a coefficient defining the strain rate sensitivity. A linear correlation allowed extrapolation of the creep prefactor (B) from fatigue data. The extrapolated values were systematically higher than the values measured directly from creep and only converged at T_g. The difference was attributed to damage of the craze fibrils during crack closure upon unloading in the fatigue cycle.

1. Introduction

Plastic pipes, particularly those manufactured from poly(vinyl chloride) (PVC) and polyethylene (PE), have been in service successfully for many years. In use, pipes usually experience constant pressure and failure mainly occurs under a static load. Testing materials under exact field conditions is impractical because of the very long failure times, and therefore prediction of long-term failure from short-term tests is desirable. The stress-lifetime approach generally used to characterize creep fracture of PVC relies on elevated stress and elevated temperature tests as a means for predicting long term behavior from short-term tests [1]. A survey of the performance of unplasticized PVC pressure pipelines shows that PVC pipes can fail in ways that are not predicted by regression data of hoop stress versus time-to-burst [2].

Fatigue testing presents another method of accelerating fracture. Numerous studies address the nature of fatigue crack propagation in PVC [3–17]. The crack growth rate expressed as the change in crack length per cycle da/dN is usually described by the conventional Paris relationship

$$\frac{da}{dN} = A\Delta K_I^m \tag{1}$$

where A and m are material constants, and ΔK_I is the change in stress intensity factor during one fatigue cycle. The prefactor A of PVC is highly dependent on formulation [3], e.g. molecular weight, plasticizer content, and amount of impact modifier. The slope m tends to be more consistent, ranging between 2.6 and 3 in most of the recent reports [4–7]. A single

*Author to whom all correspondence should be addressed.

formulation of the Paris law as given in Equation 1 does not accommodate data for PVC obtained at different frequencies. It was observed that crack growth rate da/dN increased with decreased frequency [4, 6, 8, 9]. Similarly, Equation 1 may not describe the effect of changing mean stress under constant ΔK_I. Conflicting reports found crack growth rate to either increase [8], or remain unchanged [10], with increasing mean stress.

Recently a fatigue-to-creep correlation in the kinetics of slow crack propagation was developed for polyethylene pipe resins [18–21]. The dynamic component of fatigue loading was systematically varied by decreasing frequency or amplitude. Correlation in mechanism of fatigue and creep crack propagation was inferred from the common exponent in the Paris laws for fatigue and creep, $da/dt = A_f \Delta K_I^{4.0}$ and $da/dt = B K_I^{4.0}$, respectively, and subsequently confirmed by examination of fracture surfaces. The effect of varying the dynamic component in the tension-tension mode was ascribed to the impact of strain rate on craze fibril growth and fracture. All the kinetic data could be factorized by modifying the Paris law for creep to include strain rate effects according to the relationship

$$\frac{da}{dt} = B\langle K_I^4 \rangle_T (1 + C\dot{\varepsilon}) \tag{2}$$

where $B\langle K_I^4 \rangle_T$ indicates the creep component averaged over the period T of the fatigue cycle and the term $(1 + C\dot{\varepsilon})$ is a fatigue acceleration factor that is a linear function of strain rate. The magnitude of the coefficient C defines the strain rate sensitivity. The larger C is, the higher the effect of strain rate, and, hence, the greater the fatigue acceleration.

The goal of the present work was to test the fatigue to creep correlation developed for polyethylene with another pipe material. As with polyethylene, slow crack growth in PVC proceeds through a crack-tip craze zone. However the structure of the craze zone and the manner in which the craze fractures differ considerably. In polyethylene the large damage zone consists of a main craze with a continuous membrane at the crack tip and subsidiary shear crazes that emerge from the membrane region at an angle of about 30° with respect to the primary craze [21]. Crack growth proceeds in a stepwise manner where the crack is arrested for much of the specimen fracture time. In contrast, slow crack growth in PVC pipe proceeds by continuous fracture of a single small crack-tip craze [11–13]. The kinetics and mechanism of slow crack propagation in PVC pipe in fatigue and creep loading was studied over the temperature range from ambient to 70°C. The relationship between fatigue and creep was examined by systematically decreasing the dynamic component of fatigue loading. This was accomplished by decreasing the amplitude (ratio of maximum stress intensity factor to minimum stress intensity factor) and by increasing the time duration (lower frequency) of the tension-tension fatigue cycle. The results were compared with previous observations on polyethylene.

2. Experimental

Compact tension specimens with dimensions in accordance with ASTM D 5045-93 were cut directly from PVC pipe. The M_w of the PVC pipe material was 80,000 with $M_w/M_n \sim 2$. The pipe had a 610 mm nominal diameter with a 32 mm thick wall. A hoop section was cut from the pipe and sawed in the radial direction to obtain small blocks. The blocks were machined to make a specimen of the dimensions specified previously [17]. Deviation from the plane strain condition was minimized with V-shaped side grooves. Specimens were notched in two steps: an initial 10 mm notch made with a bandsaw was extended an additional 2.5 mm with a razor blade cut made at a controlled rate of 1 μm s^{-1} at 80°C. The specimen geometry determined that the crack propagated radially with respect to the pipe wall.

Mechanical fatigue units capable of applying a very stable and accurate load (±0.5 N) were used to conduct fatigue tests. The units also operated in creep (constant load). The stress intensity factor K_I was calculated from the applied load as specified in the ASTM standard. A manual zoom macrolens attached to a video camera was used to observe crack growth. The camera was routed through a VCR and video monitor, and the experiment was recorded onto videocassette. The crack length was measured from the video.

Creep loading was approached by two series of fatigue experiments. One series was undertaken by increasing R-ratio (ratio of the minimum to the maximum stress intensity factor) from 0.1 to unity (creep). Another series of experiments was undertaken with decreasing frequency from 1.0 Hz to 0.01 Hz. All fatigue tests were conducted in the tension-tension mode. Creep tests and fatigue tests were carried out at 23°, 35°, 50°, 55°, 60°, 65°, and 70°C. The environmental chamber maintained the temperature at ±0.2°C for temperatures higher than 23°C.

Fracture surfaces were coated with 12 nm of gold and examined in a JEOL JSM 840A scanning electron microscope (SEM). The accelerator voltage was set at 5 or 10 kV and the probe current at 6×10^{-11} A to minimize radiation damage to the specimens.

Selected specimens were loaded until the crack length reached 1.5 mm, removed from the fatigue unit, and sectioned perpendicular to the crack growth plane. Some of the sections were polished, mounted in a sample holder that held the crack open, coated with 12 nm of gold and examined in the SEM to obtain the side view of the damage zone ahead of crack tip. Other sections were cryofractured in order to examine the corresponding fracture surface in the SEM.

3. Results and discussion

3.1. Paris relationship

The conventional approach for describing fatigue crack propagation was followed, and the crack growth rate was tested against the Paris law using the form

$$\frac{da}{dt} = A_f \Delta K_I^m \tag{3}$$

where the crack growth rate is expressed as da/dt, A_f and m are material constants, and ΔK_I is the

change in stress intensity factor during one fatigue cycle.

Tests were carried out at constant temperature, R-ratio and frequency with different $K_{I,\max}$. The raw data (crack length vs. time) were fit with a polynomial curve, which gave the crack growth rate ($\mathrm{d}a/\mathrm{d}t$) as the slope as shown in Fig. 1a. When the crack growth rate was plotted against ΔK_I, data from each experiment provided a series of points because the stress intensity factor difference increased as the crack grew, as shown in Fig. 1b. In each test, there was an initial period when the crack growth rate was lower than the rate of steady state propagation. This was interpreted as an initiation period during which the balance between the rates of formation and rupture of the damage zone was not fully established. Under different $K_{I,\max}$, the steady state data described a single linear relationship on a log-log plot, Fig. 1b. The slope of the Paris plot gave $m = 2.7$, which was consistent with numerous reports in the literature [3–17]. The magnitude of the crack growth rate at 23°C ($A_f = 0.1\ \mu\mathrm{m\,s^{-1}}$) also fell in the range previously reported for PVC pipe resins tested under similar conditions of temperature and ΔK_I.

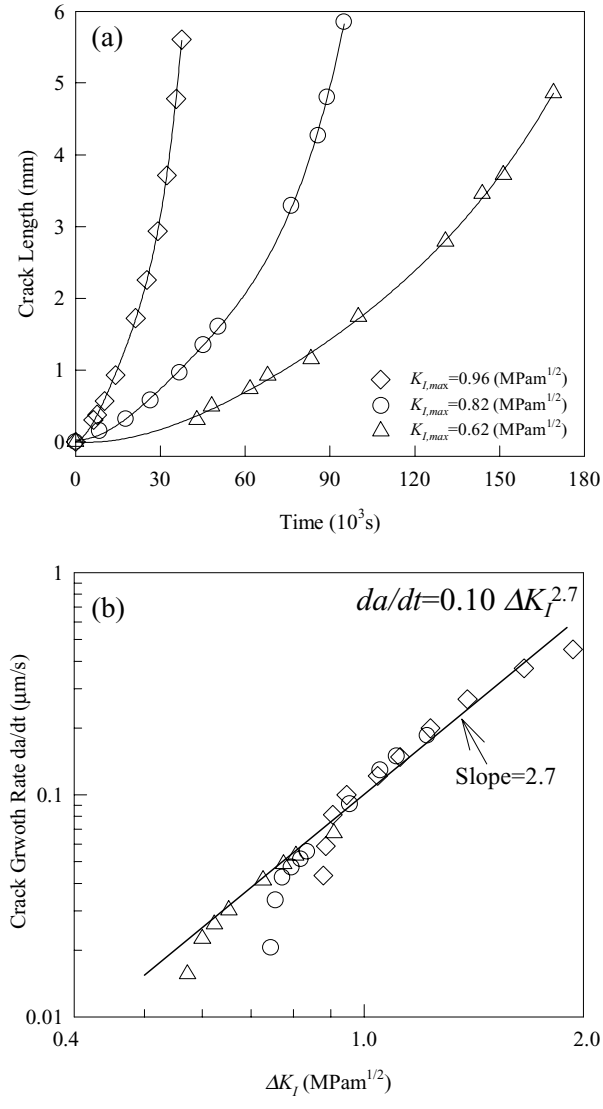

Figure 1 Effect of $K_{I,\max}$ on fatigue crack propagation in PVC pipe at 23°C, frequency 1.0 Hz and R-ratio 0.1: (a) Crack length as a function of fatigue time; and (b) Paris plot of crack growth rate.

With the same loading frequency and R-ratio, increasing temperature accelerated crack propagation as indicated by increasing prefactor A_f. In contrast, the exponent m remained constant at 2.7, as shown in Fig. 2.

Crack growth was considerably slower in creep loading than in fatigue loading, and measurements on a laboratory time scale were limited to temperatures of 50°C and higher. Creep crack propagation of PVC pipe followed the Paris law expressed as

$$\frac{\mathrm{d}a}{\mathrm{d}t} = B K_I^n \tag{4}$$

where crack growth rate is expressed as $\mathrm{d}a/\mathrm{d}t$, B and n are material constants, and K_I is the stress intensity factor, Fig. 3. In the temperature range studied, the power law dependence on K_I ($n = 2.7$) was the same as in fatigue. Conservation of the power law dependence on stress intensity factor in creep and fatigue was indicative of a common crack propagation mechanism [18–23].

The temperature dependence of crack growth rate is contained in the fatigue prefactor A_f and creep prefactor B. Plots of ln B vs. T^{-1} indicated that

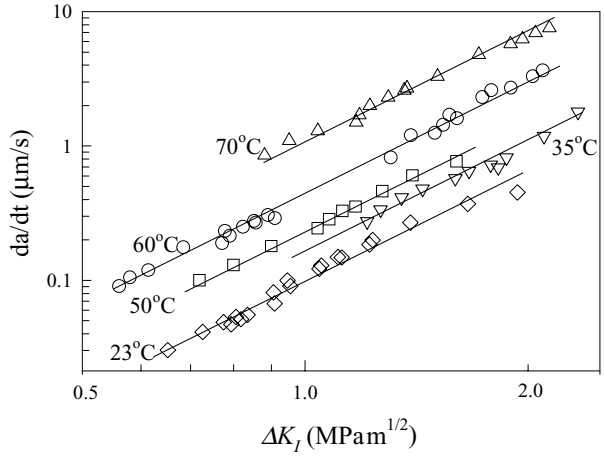

Figure 2 Effect of temperature on the Paris plot for fatigue crack propagation in PVC pipe at frequency 1.0 Hz and R-ratio 0.1.

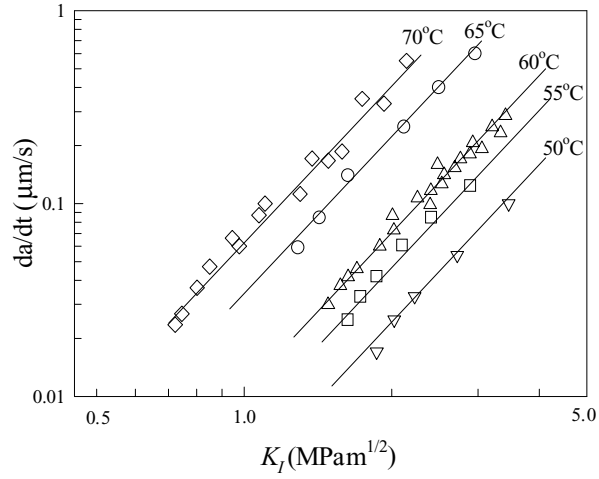

Figure 3 Effect of temperature on the Paris plot of creep crack propagation in PVC pipe.

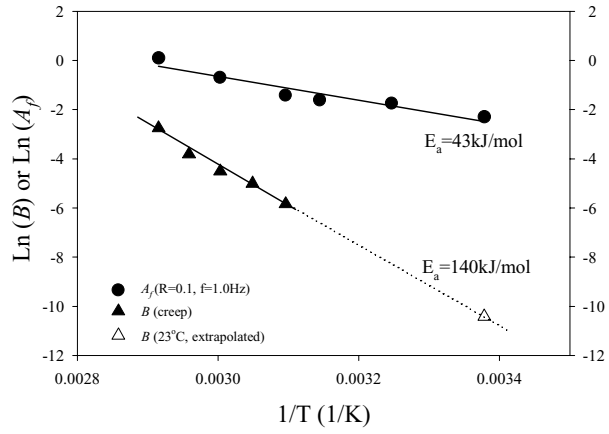

Figure 4 Arrhenius plots of the Paris law prefactor for creep and fatigue crack propagation with extrapolation to the creep prefactor at 23°C.

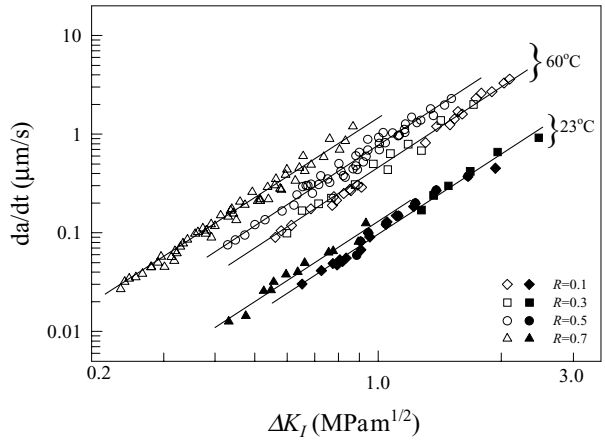

Figure 5 Effect of R-ratio on the Paris plot for fatigue crack propagation at 23°C and 60°C for frequency 1.0 Hz.

creep crack propagation rate followed an Arrhenius relationship

$$B = B_o \exp\left(\frac{-E_c}{RT}\right) \tag{5}$$

with activation energy $E_c = 140$ kJ/mol, Fig. 4. This allowed the prediction of the creep crack growth rate at 23°C. A creep experiment at 23°C is currently being carried out to test the validity of this extrapolation. The test was started in April, 2001 and a small crack was observed in Nov., 2002. The predicted failure time from Equation 5 is about 1000 days, i.e. failure should occur in January, 2004.

The temperature dependence of the fatigue prefactor A_f with $R = 0.1$, $f = 1.0$ Hz also conformed to the Arrhenius relationship

$$A_f = A_o \exp\left(\frac{-E_f}{RT}\right) \tag{6}$$

and gave activation energy $E_f = 43$ kJ/mol, which was much lower than the activation energy for creep. The activation energy for fatigue was similar to that reported previously [9, 12]. Different activation energies for fatigue and creep crack propagation indicated that fatigue and creep could not be directly correlated using the Paris law.

3.2. Fatigue approach to creep

Creep can be approached from fatigue by decreasing amplitude (increasing R-ratio) or decreasing frequency. Changing the R-ratio had very little effect on the rate of fatigue crack propagation in PVC pipe at ambient temperature with frequency 1.0 Hz, Fig. 5. Data for different R-ratios superposed within the experimental scatter except for R-ratio of 0.7. An effect of R-ratio on fatigue crack propagation rate was more apparent at 60°C. Tests at this temperature with different R-ratios could not be superposed if plotted versus ΔK_I in the fatigue cycle. The fatigue prefactor A_f increased as the R-ratio increased from 0.1 to 0.7. However, the data showed the same power law dependence ($m = 2.7$) on ΔK_I in the fatigue cycle. A similar effect of R-ratio on A_f, with conservation of the exponent m, was observed at 35°C, 45°C, 50°C and 70°C. Thus, a single formulation of the Paris law did not describe the R-ratio effect on fatigue of PVC pipe.

Decreasing the frequency from 1 Hz to 0.01 Hz under the same ΔK_I slightly increased the rate of fatigue crack propagation when crack growth rate was calculated in the usual manner as da/dN. However, to obtain comparisons with creep crack growth rates, the crack growth rate was calculated as change in crack length per unit time, da/dt. Calculated in this manner, the crack growth rate decreased with decreasing frequency. Decreasing the frequency also emphasized the effect of R-ratio on fatigue crack propagation rate as shown for data obtained at 23°C in Fig. 6. The Paris law described the data at each frequency and R-ratio with a different value of the prefactor A_f, but with the same power law dependence ($m = 2.7$). Frequency-independence of the exponent m in the Paris law characterizes fatigue crack growth in many polymers, including polyethylene [19, 20], poly(methyl methacrylate) [24, 25], polycarbonate [8], ABS [26], and polyamide-6 [27]. This feature is generally taken to indicate that the mechanism of fatigue crack propagation is the same under different frequencies.

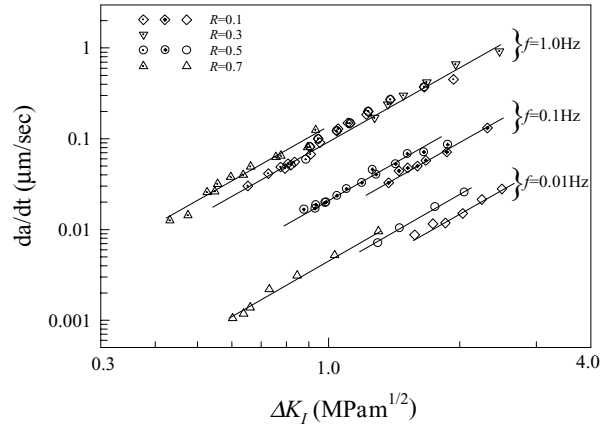

Figure 6 Effect of frequency and R-ratio on fatigue crack propagation at 23°C.

3.3. Mechanism of slow crack growth in PVC pipe

Slow crack growth in PVC reportedly proceeds by formation and fracture of a craze zone at the tip of the propagating crack [8, 13–16]. To examine the craze zone, fatigue tests at 23°C at two frequencies (1.0 Hz and 0.01 Hz) with the same $K_{I,\max}$ (1.70 MPam$^{1/2}$) and R-ratio (0.1) were interrupted in the steady state crack propagation region when the crack length reached about 1.5 mm. The specimens were sectioned through the crack-tip damage zone to obtain the SEM images in Fig. 7a and c.

The crack propagated through a pre-existing craze of highly drawn fibrils as shown in Fig. 7a. Crack propagation occurred by continuous fracture of craze fibrils at the crack tip and simultaneous lengthening of the craze damage zone. Remnants of fractured craze fibrils were left on the fracture surface, Fig. 7b. Decreasing the frequency from 1.0 Hz to 0.01 Hz retained the craze mechanism, however the density of craze fibrils increased significantly with decreased loading rate, Fig. 7c. The higher density of craze fibrils at frequency 0.01 Hz was particularly evident on the fracture surface, Fig. 7d. Nevertheless, the craze mechanism of slow crack propagation was retained. This confirmed the conclusion, drawn from the Paris plots, that correspondence in the power law dependence ($m = 2.7$) indicated that the crack propagation mechanism was preserved with different frequencies.

The sequence of micrographs in Fig. 8 shows the effect of decreasing frequency from 1.0 Hz to 0.01 Hz to creep (0 Hz) at 50°C and $K_{I,\max}$ of 1.70 MPam$^{1/2}$ on craze fibril density. Again, the fibril density increased as the frequency decreased from 1.0 Hz to 0.01 Hz, Fig. 8a and b. At this temperature, creep fracture surfaces were available for comparison. The image in Fig. 8c with many highly drawn and fractured craze fibrils closely resembled the fracture surface obtained in fatigue at 0.01 Hz. Possibly the fractured fibrils on the creep specimen were even more dense and more highly drawn. The similarity confirmed preservation of the craze fracture mechanism in creep crack propagation, as was suggested by correspondence in the Paris law exponent ($m = 2.7$).

An increase in craze fibril density with increasing temperature was evident by comparing fracture surfaces from fatigue experiments carried out at 23°C and 50°C under the same frequency, R-ratio, and $K_{I,\max}$ (compare Figs 7b and 8a, or Figs 7d and 8b).

Craze failure may occur by fracture (scission) or pullout (disentanglement) of highly oriented chains in the craze fibrils [28–31]. Chain scission is favored at lower temperature and/or higher strain rate. On the other hand, chain disentanglement is favored at higher temperature and/or lower strain rate. In fatigue crack propagation, increasing density of highly drawn craze fibrils on the fracture surface with increasing temperature and decreasing strain rate indicated the increasing contribution of chain pullout. When the strain rate in fatigue was low enough, disentanglement dominated and the fatigue fracture surface closely resembled that of creep fracture where the strain rate was essentially zero. This is illustrated by the 50°C fracture surfaces for fatigue with frequency 0.01 Hz and creep (Fig. 8b and c).

3.4. Strain rate approach for correlating fatigue and creep crack growth in PVC pipe

The role of creep in fatigue crack propagation was examined previously by considering fatigue crack growth to consist of two components: the crack growth due to creep and the crack growth due to true fatigue. The methodology was developed for discontinuous crack propagation where the crack was arrested for much of the specimen fracture time [18–21]. In this case, the creep rate under variable tensile stress was determined by the transient magnitude of the load. However,

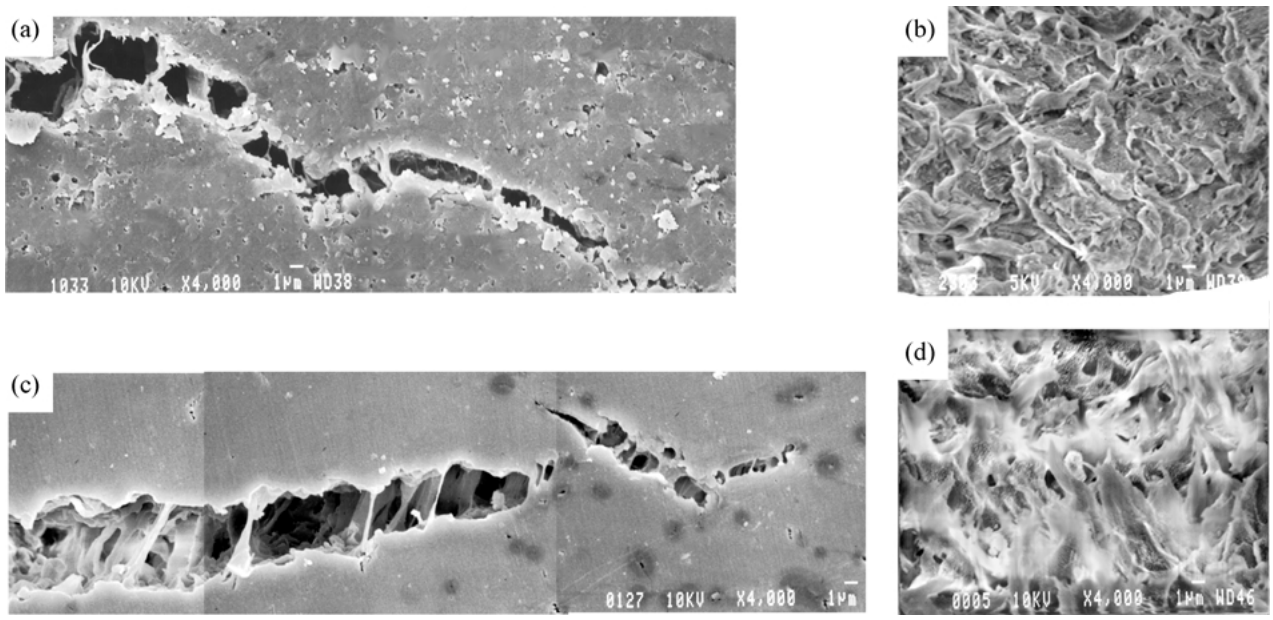

Figure 7 Effect of frequency on the crack-tip craze in fatigue at 23°C for R-ratio 0.1 and $K_{I,\max}$ 1.70 MPa m$^{1/2}$: (a) Craze at frequency 1.0 Hz; (b) fracture surface at frequency 1.0 Hz; (c) craze at frequency 0.01 Hz; and (d) fracture surface at frequency 0.01 Hz.

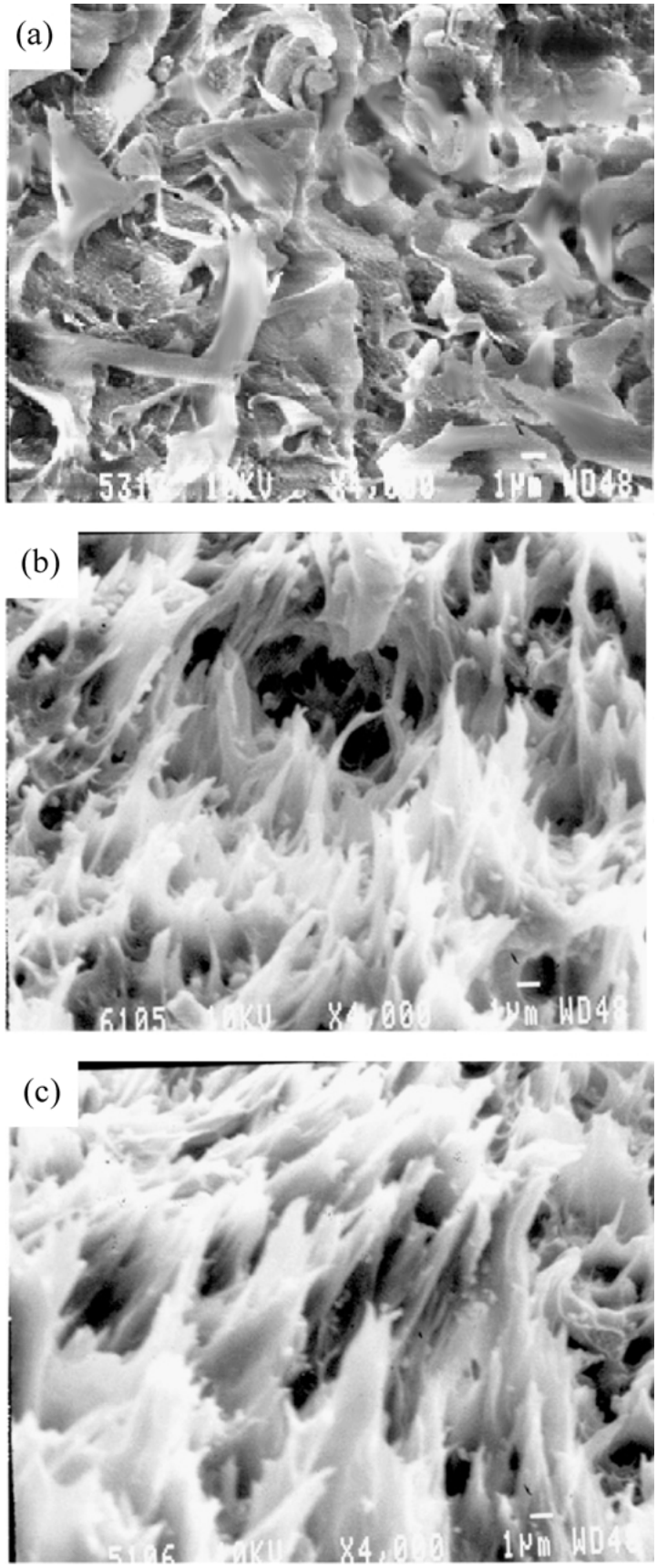

Figure 8 Effect of loading rate on the fracture surface at 50°C for $K_{I,\max}$ 1.70 MPa $m^{1/2}$: (a) Fatigue at frequency 1.0 Hz and R-ratio 0.1; (b) fatigue at frequency 0.01 Hz and R-ratio 0.1; and (c) creep.

crack growth in PVC pipe is continuous [11–13], and the creep rate is determined by the maximum load as $BK_{I,\max}^{2.7}$.

As regards the parameters that affect fatigue acceleration, R-ratio determines the amplitude of the load oscillations and frequency defines their time scale. Because the periodic deformation of the craze ahead of the crack tip monotonically follows the load, both parameters primarily impact the strain rate. Thus, the origin of fatigue crack growth acceleration lies in strain rate

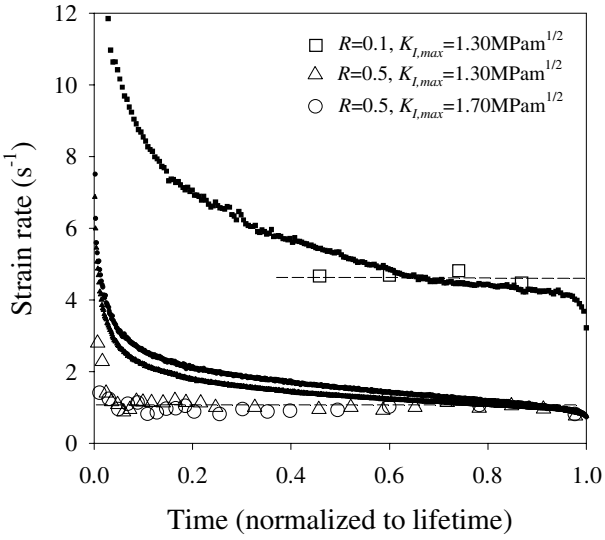

Figure 9 Comparison of remote strain rate (solid symbols) and local strain rate (open symbols) during fatigue crack propagation at 60°C and frequency 1.0 Hz.

effects. Therefore, crack growth rate in fatigue can be characterized by a contribution from the creep process multiplied by a fatigue acceleration factor β that is a function of strain rate only

$$\frac{da}{dt} = B_f K_{I,\max}^{2.7} \beta(\dot{\varepsilon}) \tag{7}$$

where B_f replaces the experimentally determined creep prefactor (B), which was only available for temperatures of 50°C or higher.

The strain rate at the crack tip in fatigue was measured in two ways: from cross-head displacement and from notch-tip opening. The former gave the remote strain rate, whereas the latter was a more direct measure of the local strain rate at the crack tip. A comparison of the two methods was made for several loading conditions, as shown in Fig. 9. For a given loading condition, the local strain rate did not change significantly during the fatigue lifetime. In comparison, the remote strain rate was initially much higher than the local strain rate, however it decreased as the crack propagated until it converged to the local strain rate at 70–90% of the fatigue lifetime. This roughly coincided with the region of steady state crack propagation that defined the Paris relationship. The examples in Fig. 9 demonstrate that for a given frequency, R-ratio and temperature, strain rate at the crack tip did not depend on $K_{I,\max}$. In contrast, R-ratio had a large effect on strain rate, which decreased from 4 s^{-1} to 1 s^{-1} as R-ratio increased from 0.1 to 0.5 for the temperature and frequency illustrated.

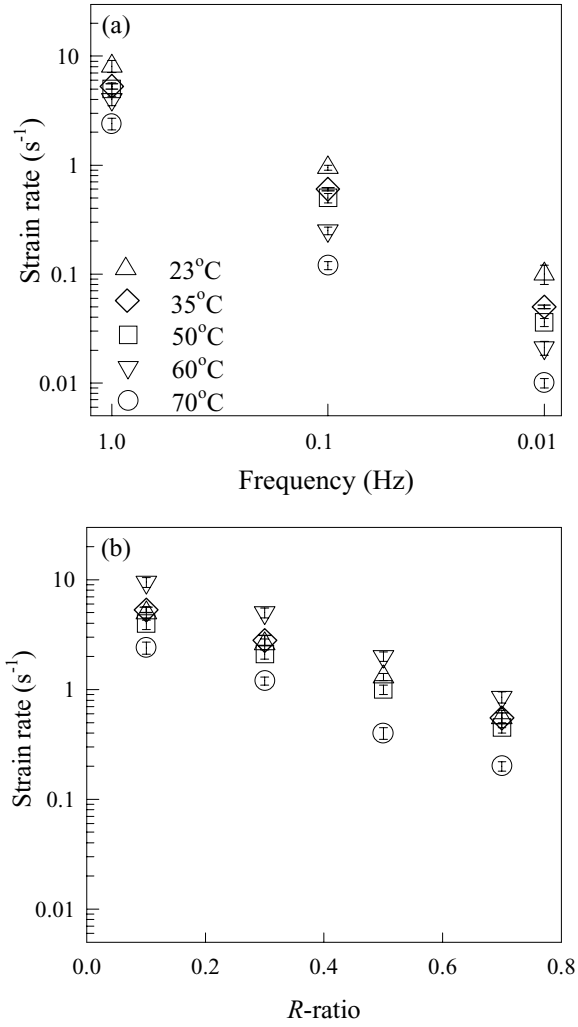

Figure 10 Strain rate in fatigue: (a) Effect of frequency; and (b) effect of R-ratio.

The remote strain rate was more easily accessed experimentally than the local strain rate. In experiments where the strain rate at the crack tip was not measured directly, the average remote strain rate between 70% and 90% of the fatigue lifetime was taken as the strain rate at the crack tip, Table I. The dependence of strain rate on frequency and R-ratio for various temperatures is shown in Fig. 10. The strain rate was approximately proportional to frequency. Increasing R-ratio (decreasing amplitude) from 0.1 to 0.7 decreased the strain rate by approximately a factor of 10. Increasing temperature from 23°C to 70°C resulted in a decrease of strain rate by a factor of five.

The Paris plots for fatigue (e.g. Figs 2, 5, and 6) were constructed from data obtained under conditions of

TABLE I Effect of loading conditions on strain rate during fatigue crack propagation of PVC pipe

	Strain rate (s^{-1}) for $R = 0.1$			Strain rate (s^{-1}) for $f = 1.0$ Hz			
Temperature (°C)	$f = 1.0$ Hz	$f = 0.1$ Hz	$f = 0.01$ Hz	R 0.1	R 0.3	R 0.5	R 0.7
23	8.1	0.95	0.10	8.1	4.0	1.6	0.70
35	5.3	0.60	0.050	5.3	2.8	–	0.55
50	5.0	0.50	0.024	5.0	2.6	1.3	0.55
60	4.0	0.25	0.021	4.0	2.1	1.0	0.45
70	2.4	0.12	0.010	2.4	1.2	0.40	0.20

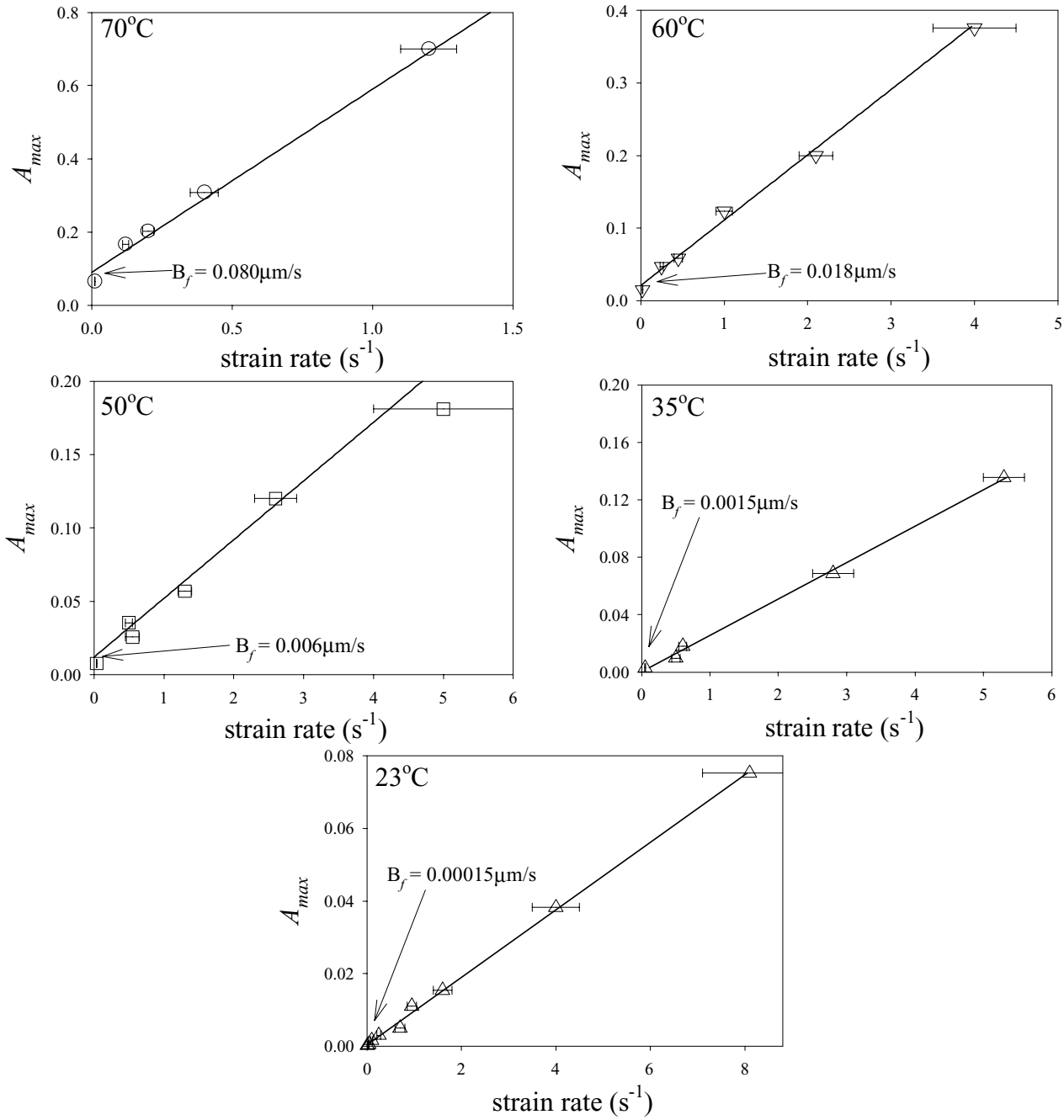

Figure 11 Relationship between strain rate and fatigue prefactor expressed as $A_{\max} = A_f(1-R)^{2.7}$ at various temperatures.

constant frequency, R-ratio and temperature, and therefore each Paris plot corresponded to a constant strain rate experiment. Noting that $\Delta K_I = (1-R)K_{I,\max}$, the conventional Paris law (Equation 3) for fatigue of PVC was rewritten as

$$\frac{\mathrm{d}a/\mathrm{d}t}{K_{I,\max}^{2.7}} = A_{\max} \tag{8}$$

where $A_{\max} = A_f(1-R)^{2.7}$. The effect of strain rate on crack growth rate is shown in Fig. 11 with $A_{\max}$ plotted against strain rate for all tests with different R-ratio and different frequency. For each temperature, all the data fell on the same line, which confirmed that fatigue acceleration depended only on strain rate. From the data in Fig. 11, an expression for β was obtained where $\beta = (1 + C\dot{\varepsilon})$. Therefore, crack growth rate in fatigue can be described as the product of a creep contribution and a fatigue acceleration factor that is a function of strain rate only

$$\frac{\mathrm{d}a}{\mathrm{d}t} = B_f K_{I,\max}^{2.7}(1 + C\dot{\varepsilon}) \tag{9}$$

where the parameters B_f and C are obtained from the linear plots in Fig. 11. The limitations to Equation 9 are that R-ratio must be greater than zero to avoid compressive damage to craze fibrils and that the crack growth mechanism must be conserved over fatigue and creep loading conditions.

The strain rate sensitivity parameter C indicates how strongly fatigue accelerates the rate of crack growth compared to creep. The effect of temperature on C is given in Table II. It is seen that fatigue is much more effective in accelerating crack growth in PVC pipe at lower temperatures than at higher temperatures

TABLE II Effect of temperature on the strain rate sensitivity (C) in PVC fatigue crack propagation

Material	Temperature (°C)	C (s)
PVC	23	60
	35	17
	50	7
	60	6
	70	6

TABLE III Effect of R-ratio and frequency on A_{max} for fatigue crack propagation of PVC pipe

Temperature (°C)	$R = 0.1$, $f = 0.1$ Hz		$R = 0.7$, $f = 1.0$ Hz	
	$\dot{\varepsilon}$ (s^{-1})	A_{max} ($\mu m \cdot s^{-1}$)	$\dot{\varepsilon}$ (s^{-1})	A_{max} ($\mu m \cdot s^{-1}$)
23	0.95	0.011	0.70	0.0050
35	0.60	0.018	0.55	0.0097
50	0.50	0.035	0.55	0.026
60	0.25	0.047	0.45	0.058
70	0.12	0.17	0.20	0.20

approaching the T_g. As a consequence, fatigue crack growth rate is readily measured over the entire temperature range including ambient temperature, although it is practical to measure creep crack growth in the laboratory only at higher temperatures.

At the molecular level, the entanglement loss that leads to deterioration of craze fibrils occurs by a combination of chain disentanglement and main chain scission. Craze failure in creep is ascribed primarily to chain disentanglement by the processes of chain slippage and pullout. When the temperature is well below T_g disentanglement is very slow and the time to creep failure is very long. Fatigue accelerates deterioration of craze fibrils by enhancing the rate of chain scission. This imparts a dramatic increase in crack growth at lower temperatures, which is apparent in large values of C. As the temperature is increased the rate of chain disentanglement is expected to increase faster than the rate of chain scission [30, 31]. Chain pullout becomes the predominant mechanism of entanglement loss in both creep and fatigue. Under these conditions fatigue does not strongly accelerate failure compared to creep and the parameter C is small.

The extrapolated creep prefactor from fatigue (B_f) and the prefactor measured directly from creep (B) are compared in Fig. 12. The extrapolated value was systematically higher than the measured value until they converged at 80°C, which is the T_g of PVC. Inequality of B_f and B implied the existence of a fatigue acceleration factor in addition to the strain rate contribution. Damage of craze fibrils during crack-tip closure in the unloading portion of the fatigue cycle was a possible

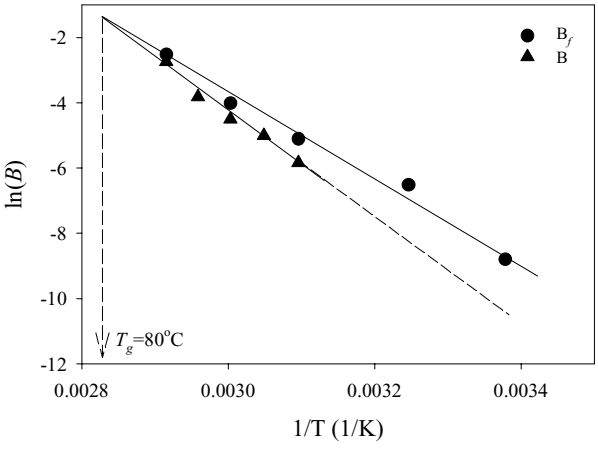

Figure 12 Comparison of creep prefactor extrapolated from fatigue (B_f) with measured creep prefactor (B).

cause of the difference between B_f and B even though specimens were in tension throughout the fatigue cycle [32, 33]. Because drawn craze fibrils have practically no recovery, fibrils were compressed and bent during crack tip closure. With increasing temperature, chains became more flexible and craze fibrils experienced less damage during crack tip closure until at T_g chain flexibility was high enough that crack tip closure did not damage the craze fibrils and B_f converged with B.

Other evidence that damage of craze fibrils during crack tip closure affected the measured crack growth rate was found by comparing fatigue tests performed at approximately the same strain rate but with different loading conditions. As indicated in Table III approximately the same strain rate was achieved with two different conditions of R-ratio and frequency: higher amplitude with lower frequency ($R = 0.1$, $f = 0.1$ Hz) and lower amplitude with higher frequency ($R = 0.7$, $f = 1.0$ Hz). Despite the generally good correlation between A_{max} and strain rate in Fig. 11, A_{max} was slightly but consistently higher for the higher amplitude $R = 0.1$, $f = 0.1$ Hz condition, particularly in tests at lower temperatures (23°, 35°, and 50°C). This difference was attributed to additional damage sustained by the fibrils during crack tip closure under the lower R-ratio condition.

Previous studies that examined the effect of frequency on fatigue crack propagation generally report the crack growth rate as da/dN. Measured in this way, the fatigue crack growth rate of some thermoplastics including polycarbonate, polysulfone, and polyamide-66 was found to be insensitive to frequency (ambient temperature, constant R-ratio) with the same power law dependence m for all frequencies. If the results for these polymers are considered in terms of Equation 9 with crack speed as da/dt, it means that A_{max} is essentially proportional to strain rate, which only occurs if the product $C\dot{\varepsilon}$ in Equation 9 is large compared to unity. Under these conditions, the creep prefactor cannot be reliably obtained from extrapolation of fatigue results using Equation 9. It would appear that these polymers have large C, i.e. the strain rate sensitivity of crack growth at ambient temperature is high. In order to reliably predict creep from fatigue, it is essential that fatigue tests be performed under conditions of frequency and R-ratio that ensure a significant creep contribution to the overall crack growth rate. This was achieved previously with MDPE and HDPE, and in this study with PVC.

4. Conclusions

Kinetics of fatigue and creep crack propagation in PVC pipe followed the Paris law with the same power law dependence on stress intensity factor, $da/dt = A_f \Delta K_I^{2.7}$ and $da/dt = B K_I^{2.7}$, respectively. Although the simple Paris law was inadequate for correlating fatigue to creep crack propagation in PVC pipe, conservation of the exponent 2.7 provided evidence that the mechanism of slow crack growth was the same in fatigue and creep. Examination of crack-tip damage zones and post-failure fracture surfaces confirmed the mechanism as continuous crack growth through a crack-tip craze. The density of drawn craze fibrils decreased with decreased temperature or increased frequency. Fatigue was seen as accelerating craze deterioration by enhancing the rate of chain scission. Fatigue loading was most effective in accelerating crack growth at low temperatures where the rate of chain pullout was very slow. At higher temperatures chain pullout became the predominant mechanism of entanglement loss in both creep and fatigue, and consequently fatigue was less effective for accelerating crack growth. At each temperature, the fatigue acceleration effect depended only on strain rate in the fatigue cycle. Therefore crack growth rate could be modeled as the product of a creep contribution that depended only the maximum stress intensity factor and a fatigue contribution that depended on strain rate. This extends an approach developed previously for high density polyethylene and a medium density polyethylene pipe resin. This may be a general approach that is applicable to slow crack growth in other engineering thermoplastics.

Acknowledgments

This project was made possible through the generous financial support of EPIC.

References

1. K. GOTHAM and M. HITCH, *Pipes & Pipelines International* **20** (1975) 10.
2. D. MOORE, R. STEPHENSON and M. WHALE, *Plastics, Rubber and Composites Processing and Applications* **3** (1983) 53.
3. M. SKIBO, J. MANSON, R. HERTZBERG and E. COLLINS, *J. Macromol. Sci.-Phys.*, B **14**(4) (1977) 525.
4. L. BURN, *Plastics, Rubber and Composites Processing and Applications* **21** (1994) 99.
5. L. KONCZOL, W. DOLL and L. BEVAN, *Colloid & Polymer Science* **268** (1990) 814.
6. H. KIM and X. WANG, *J. Mater. Sci.* **29** (1994) 3209.
7. S. MADDOX and S. MANTEGHI, *Plastics, Rubber and Composites Processing and Applications* **17** (1992) 5.
8. R. HERTZBERG and J. MANSON, in "Fatigue of Engineering Plastics" (Academic Press, New York, 1980).
9. J. PHILLIPS, R. HERTZBERG and J. MANSON, in "Fatigue '87," vol. III (Engineering Materials Advisory Service LTD, West Mildland, UK, 1987) p. 1317.
10. H. KIM, R. TRUSS, Y. MAI and B. COTTERELL, *Polymer* **29** (1988) 268.
11. J. MANDELL and J. CHEVAILLIER, *Polym. Engr. Sci.* **25** (1985) 170.
12. Y. MAI and P. KEER, *J. Vinyl. Technology* **7** (1985) 130.
13. L. LEE, J. MANDELL and F. McGARRY, *Polym. Engr. Sci.* **26** (1986) 626.
14. C. RIMNAC, R. HERTZBERG and J. MANSON, *J. Mater. Sci.* **19** (1984) 1116.
15. M. SCHINKER, L. KONCZOL and W. DOLL, *J. Mater. Sci. Lett.* **1** (1982) 475.
16. W. DOLL, in "Fractography and Failure Mechanisms," edited by A. Roulin-Moloney (Applied Science, London, 1989) p. 387.
17. Y. HU, J. SUMMERS, A. HILTNER and E. BAER, *J. Vinyl. and Addit. Technology* **8**(4) (2002).
18. M. PARSONS, E. STEPANOV, A. HILTNER and E. BAER, *J. Mater. Sci.* **34** (1999) 3315.
19. *Idem., ibid.* **35** (2000) 1857.
20. *Idem., ibid.* **35** (2000) 2659.
21. *Idem., ibid.* **36** (2001) 5747.
22. N. BROWN and X. LU, *Polymer* **36** (1995) 543.
23. P. O'CONNELL, M. BONNER, R. DUCKETT and I. WARD, *ibid.* **36** (1995) 2355.
24. B. MUKHERJEE and D. BURNS, *Exp. Mech.* **11** (1971) 433.
25. W. CHENG, G. MILLER, J. MANSON, R. HERTZBERG and L. SPERLING, *J. Mater. Sci.* **25** (1990) 1924.
26. H. KIM and X. WANG, *J. Appl. Polym. Sci.* **57** (1995) 811.
27. M. WYZGOSKI, G. NOVAK and D. SIMON, *J. Mater. Sci.* **25** (1990) 4501.
28. H. BROWN, *Macromolecules* **24** (1991) 2752.
29. C. PLUMMER and A. DONALD, *Polymer* **32** (1991) 409.
30. E. KRAMER and L. BERGER, in "Advances in Polymer Science: Crazing in Polymers," 91/92:2, edited by H. Kause (Springer-Verlag, New York, 1990) p. 1.
31. L. BERGER and E. KRAMER, *Macromolecules* **20** (1987) 1980.
32. H. BROWN, E KRAMER and R. BUBECK, *J. Polym. Sci.: Part B: Polym. Phys.* **25** (1987) 1765.
33. R. SCHIRRER, *J. Mater. Sci.* **22** (1987) 2289.

Received 18 September
and accepted 24 October 2002